*The Canadian Mineralogist*
Vol. 36, pp. 483-496 (1998)

# RUBIDIUM FELDSPARS IN GRANITIC PEGMATITES

DAVID K. TEERTSTRA, PETR ČERNÝ[1] AND FRANK C. HAWTHORNE[1]

*Department of Geological Sciences, University of Manitoba, Winnipeg, Manitoba R3T 2N2*

## ABSTRACT

Rubidium feldspars form under low-temperature conditions in the interior zones of many pollucite-bearing rare-element granitic pegmatites. The (K–Rb)-feldspars lie close to the $KAlSi_3O_8$ – $RbAlSi_3O_8$ join and have up to 26.2 wt.% $Rb_2O$ (91 mol.% Rbf) and 1.5 wt.% $Cs_2O$ (3 mol.% Csf). Three subsolidus processes generate rubidium feldspars at a microscopic scale: exsolution from a primary (K,Na,Rb)-feldspar, solution – reprecipitation from the same precursor, and metasomatic coprecipitation with K-feldspar in pollucite. (i) Near-complete exsolution and phase separation of albite and (Rb,K)-feldspar are typical of a (K,Na,Rb)-feldspar precursor with up to 5 mol.%$\square Si_4O_8$, whereas (K,Rb)-feldspar with integral stoichiometry exsolves a Rb-enriched phase only rarely. Exsolution of the (Rb,K)-feldspar postdates that of albite because the rate of diffusion of Na is greater than that of Rb; however, migration of *M*-site vacancies apparently enhances rates of Rb diffusion. Rubidium feldspar coherent with microcline is ordered and triclinic. (ii) Aggregates of microporous adularian K-feldspar + (Rb,K)-feldspar are formed by solution – reprecipitation from a Rb-bearing precursor under low-temperature deuteric conditions. (iii) Adularian (Rb,K)-feldspar also coprecipitates with end-member K-feldspar (± cookeite), in metasomatic reactions of hydrothermal fluid with early Rb-bearing feldspar and pollucite at ~300 to 150°C. Such adularian feldspar typically is untwinned, monoclinic and disordered. A broad solvus must extend between K-feldspar ($Or_{\sim 100}$) and Rb-feldspar ($Rbf_{\sim 80}$), cresting below 400°C. Feldspars with a heterogeneous distribution of K and Rb in the range $Rbf_{50}$ to $Rbf_{70}$ are common, but are probably metastable, preserved because of a slow rate of diffusion of Rb at low temperature. Compositional heterogeneity of the secondary (K–Rb)-feldspars on a microscopic scale also implies disequilibrium and arrested reactions.

*Keywords*: rubidium feldspar, potassium feldspar, microcline, sanidine, rubicline, granitic pegmatite, rubidium.

## SOMMAIRE

Le feldspath rubidique se forme à faible température, dans les zones internes de plusieurs massifs de pegmatite granitique à éléments rares et à pollucite. Ces compositions de feldspath-(K–Rb) se situent près de la série $KAlSi_3O_8$ – $RbAlSi_3O_8$, et peuvent contenir jusqu'à 26.2% de $Rb_2O$ et 1.5% de $Cs_2O$ (en poids), soit 91% Rbf et 3% Csf (base molaire). Trois processus subsolidus sont responsables de la formation de feldspath rubidique à l'échelle microscopique: exsolution à partir d'un feldspath primaire à (K,Na,Rb), solution et reprécipitation à partir d'un même précurseur, et coprécipitation au cours de la métasomatose du feldspath potassique inclus dans la pollucite. (i) Une exsolution quasi-complète et une séparation en albite et feldspath-(Rb,K) sont typiquement atteintes aux dépens du précurseur, le feldspath-(K,Na,Rb), contenant jusqu'à 5% du pôle $\square Si_4O_8$ (base molaire), tandis que le feldspath-(K,Rb) ayant une stoechiométrie intégrale ne montre que très rarement une exsolution d'un feldspar enrichi en Rb. L'exsolution du feldspath-(Rb,K) est postérieur à l'exsolution de l'albite vu le taux de diffusion plus rapide du Na que du Rb; toutefois, la migration des lacunes du site *M* favoriserait le taux de diffusion du Rb. Le feldspath rubidique en continuité cohérente avec le microcline est ordonné et triclinique. (ii) Des agrégats de feldspath potassique microporeux à morphologie d'adulaire + feldspath-(Rb,K) se sont formés par solution et reprécipitation à partir d'un précurseur rubidique à faible température au cours de réactions deutériques. (iii) Un feldspath-(Rb,K) à morphologie d'adulaire est aussi coprécipité avec le feldspath potassique pur (± cookeïte) dans des réactions métasomatiques impliquant le fluide hydrothermal, le feldspath rubidique précoce et pollucite entre environ 300 et 150°C. Ce type de feldspath est typiquement non maclé, monoclinique et désordonné. Un solvus étendu doit séparer le feldspath potassique ($Or_{\sim 100}$) et le feldspath rubidique ($Rbf_{\sim 80}$), avec un sommet inférieur à 400°C. Les grains de feldspaths qui font preuve d'hétérogénéités dans la distribution du K et du Rb dans l'intervalle $Rbf_{50}$ – $Rbf_{70}$ sont répandus, et probablement métastables vu le taux très faible de diffusion du Rb à basse température. L'hétérogénéité dans la composition du feldspath-(K–Rb) secondaire sur une échelle microscopique impliquerait un écart à l'équilibre et des réactions non complétées.

(Traduit par la Rédaction)

*Mots-clés*: feldspath rubidique, feldspath potassique, microcline, sanidine, rubicline, pegmatite granitique, rubidium.

[1] *E-mail addresses*: cernyp@ms.umanitoba.ca, frank_hawthorne@umanitoba.ca

## INTRODUCTION

Rubidium-rich feldspar has rarely been described in the literature. A high Rb content occurs in K-feldspar from granitic pegmatites of the rare-element class, and particularly in the highly fractionated, complex, pollucite-bearing pegmatites of the LCT family [peraluminous, Li,Cs,Ta-enriched; *cf.* Černý (1991) for classification]. These pegmatites attain a high degree of rare-alkali enrichment in general, and of Rb in primary K-feldspar in particular. However, even the most Rb-enriched, blocky, perthitic alkali feldspar in the late-crystallizing core-margins and cores of zoned pegmatites does not usually contain more than ~2 to 4 wt.% $Rb_2O$ (~6 to 12 mol.% Rbf; Černý 1994). The highest Rb content to date, 5.87 wt.% $Rb_2O$, was reported from the microcline phase of blocky perthitic alkali feldspar from the pollucite-bearing Red Cross Lake pegmatites, in northern Manitoba (Černý *et al.* 1985, Černý 1994). The low level of enrichment in Rb indicates that even the most advanced igneous differentiation cannot generate a Rb-dominant feldspar. However, Rb-dominant feldspars are readily produced in the triclinic, (Al,Si)-ordered form by cation exchange from albite or microcline (Wietze & Viswanathan 1971, Pentinghaus & Henderson 1979, McMillan *et al.* 1980), or as highly disordered phases by hydrothermal synthesis (Ghélis & Gasperin 1970, Gasperin 1971, Bruno & Pentinghaus 1974, Voncken *et al.* 1993).

During a systematic study of pollucite and products of its alteration, we have discovered numerous occurrences of late alkali feldspar remarkably enriched in Rb, locally grading into phases with Rb dominant over K. To date, we have mentioned the presence of these feldspars only in describing alteration of pollucite (Teertstra *et al.* 1993, 1996b, Teertstra & Černý 1995, 1997), and in conference abstracts (Teertstra & Černý 1993, 1994, Teertstra *et al.* 1996a). The only detailed accounts concern Rb-rich feldspars from the Kola Peninsula (Teertstra *et al.* 1997) and the first description of rubicline, the Rb-analogue of microcline (Teertstra *et al.* 1998a). However, our present study covered Rb-rich to Rb-dominant feldspars from thirty-three localities that provided sufficient information for genetic generalizations. Here, we present a review of modes of formation of rubidium-rich potassic feldspars and associated mineral assemblages.

## SAMPLES EXAMINED

Feldspars associated with pollucite were examined from seventy bodies of granitic pegmatite worldwide. Appreciable enrichment of feldspars in Rb was recognized at thirty-three localities: Rb-dominant feldspars were found at twelve localities, and K-dominant but Rb-rich feldspars were found in the other twenty-one pegmatites. Paragenetic and textural features of the Rb-rich to Rb-dominant feldspars show that they are of late, low-temperature origin, formed at the expense of pre-existing magmatic minerals. The Rb-enriched feldspars are very widespread locally; however, they occur on a microscopic scale, and can be recognized only by using back-scattered electron imagery and an electron microprobe. At each locality, Rb-enriched feldspars were found in one or more of the following assemblages: (1) blocky perthitic microcline associated with pollucite, (2) veins of nonperthitic microcline that cross-cut pollucite, and (3) clusters of adularia-type feldspar dispersed in pollucite. Table 1 lists the localities and summarizes information on the Rb concentrations in the (K>Rb)-feldspar precursor and in the three types of Rb-enriched feldspar.

## EXPERIMENTAL

For the feldspars from each locality, 15 to 60 compositions were determined on 3 to 25 thin sections prepared from 2 to 14 hand specimens. The chemical composition of individual phases of the feldspar was determined using wavelength-dispersion (WDS) analysis on a CAMECA SX–50 electron microprobe (EMP) operating at 15 kV and 20 nA, with a beam diameter of 5 μm. Concentrations of major elements were measured using a glass of $Rb_2ZnSi_5O_{12}$ composition (Rb$L\alpha$) and gem sanidine from Volkesfeld, Eifel, Germany (K$K\alpha$, Al$K\alpha$, Si$K\alpha$). Data were reduced using the *PAP* procedure of Pouchou & Pichoir (1985). The composition of the sanidine chip selected as a standard was optimized to agree with ideal feldspar stoichiometry by the procedure of Teertstra *et al.* (1998b). The accuracy of our results is less than 2% relative, and the precision (4σ) is approximately 1%. Minor elements were measured using albite (Na$K\alpha$), pollucite (Cs$L\alpha$), fayalite (Fe$K\alpha$), barite (Ba$L\beta$), $SrTiO_3$ (Sr$L\alpha$) and $VP_2O_5$ (P$K\alpha$). The elements Mg, Ti, F, Mn, Ga, Ca and Pb were sought but not detected in any generation of feldspar.

Feldspar formulae were calculated on the basis of 8 atoms of oxygen per formula unit (*apfu*). Monovalent and divalent cations were assigned to the *M* site, and higher-valency cations were assigned to the *T* site of the general formula $MT_4O_8$. EMP analysis of P-rich feldspar shows an $AlPSi_{-2}$ substitution (London *et al.* 1990). To adjust for this substitution, the framework charge was calculated as $TO_2^- = (Al–P)$ for comparison with the *M*-cation charge, and Si was modified using Si + 2P (where 2P indicates P + P equivalent of Al) for comparison with the monovalent *M* cations. Compositional vectors in Figures 2A, B, 4A, B, and 6A, B (see below) correspond to (1) a plagioclase-type substitution $M^{2+}Al(M^{1+}Si)_{-1}$, (2) silica substitution $\square Si(KAl)_{-1}$ expressed in the text as $\square Si_4O_8$, and (3) substitution by light-element *M*-cations whose concentration cannot be established by EMP methods. Molar percentages of end-member feldspars were calculated

TABLE 1. $Rb_2O$ CONCENTRATIONS IN THE K-PHASE OF MICROCLINE PRECURSORS AND IN THE LATE (K-Rb) FELDSPARS FROM POLLUCITE-BEARING PEGMATITES

| | wt.% $Rb_2O$ in blocky and *vein* microcline | | maximum $Rb_2O$, Rbf in late feldspars | |
|---|---|---|---|---|
| Locality | mean | (range) | wt.% $Rb_2O$ | mol.% Rbf |
| Tanco, Manitoba | 2.68 | (2.0-3.2) | 3.52 | 11 |
| | *3.25* | *(1.8-8.3)* | *24.84* | *84* |
| Red Cross Lake, Manitoba | 4.94 | (4.0-6.0) | 6.13 | 19 |
| | | | **24.37** | **83** |
| High Grade Dyke, Manitoba | *3.21* | *(2.0-4.0)* | *23.46* | *78* |
| | | | **24.07** | **82** |
| Tot Lake, Ontario | 2.77 | (1.8-4.3) | 6.65 | 20 |
| | | | **16.32** | **53** |
| Rubellite Dyke, Ontario | 3.44 | (2.8-4.9) | 13.44 | 43 |
| | | | **22.00** | **74** |
| Valor, Quebec | | | **8.86** | **27** |
| Tamminen quarry, Greenwood, Maine | *1.24* | *(0.6-1.8)* | *1.87* | *7* |
| Old Tom quarry, Greenwood, Maine | | | **13.33** | **42** |
| Norway 1, Maine | 0.66 | (0.5-0.8) | 0.80 | 2 |
| | | | **2.29** | **7** |
| Norway 2, Maine | *1.24* | *(0.6-1.8)* | *1.78* | *6* |
| | | | **2.29** | **8** |
| Walden, Connecticut | | | **2.24** | **8** |
| Leominster, Massachusetts | | | **0.47** | **2** |
| Tin Mountain, South Dakota | | | **19.24** | **64** |
| Himalaya Mine, California | | | **3.45** | **11** |
| Viitaniemi, Finland | *0.68* | *(0.6-0.7)* | *0.77* | *3* |
| | | | **2.08** | **6** |
| Luolamäki, Finland | *3.33* | *(1.5-5.9)* | *26.02* | *89* |
| | | | **20.95** | **70** |
| Nyköpingsgruvan, Utö, Sweden | | | **10.09** | **31** |
| Sušice, Czech Republic (CR) | | | **0.24** | **1** |
| Nová Ves u Českého Krumlova (CR) | 0.71 | | 0.71 | 3 |
| San Piero in Campo, Elba, Italy | *1.98* | *(0.9-3.4)* | *25.48* | *87* |
| | | | **22.70** | **75** |
| Kola Peninsula, Russia | *8.25* | *(6.5-9.2)* | *9.80* | *31* |
| | | | **26.12** | **87** |
| Eastern Siberia, Russia | 2.37 | | 2.37 | 7 |
| Mongolian Altai #1, China | *2.04* | | *2.04* | *7* |
| Mongolian Altai #3, China | | | **1.19** | **4** |
| Mongolian Altai #83, China | 1.51 | (1.3-1.7) | 1.73 | 6 |
| Morrua Mine, Mozambique | | | **19.81** | **66** |
| Bikita, Zimbabwe | | | **9.57** | **28** |
| Benson #1, Zimbabwe | 3.60 | (2.8-4.4) | 4.45 | 15 |
| Helikon, Namibia | 1.12 | (1.1-8.5) | 8.55 | 27 |
| | | | **6.02** | **19** |
| Ambatofinondrahana, Madagascar | *0.77* | | *0.77* | *3* |
| | | | 1.26 | 4 |

The K-phase of blocky and *vein* microcline and their Rb-enriched derivatives are indicated by normal type and *italics*, respectively; **adularian** (K-Rb)-feldspar is indicated by **boldface**.

according to the partial occupancy of the *M* site by each cation: thus $(Na_{0.03}K_{0.41}Rb_{0.52}Cs_{0.02})_{0.98}Al_{0.98}Si_{3.02}O_8$ has 3 mol.% albite ($Ab_3$), 41 mol.% K-feldspar ($Or_{0.41}$), 52 mol.% Rb-feldspar ($Rbf_{52}$), 2 mol.% of a hypothetical end-member Cs-feldspar ($Csf_2$) and 2 mol.% $\square Si_4O_8$. Observations made using X-ray diffraction (XRD) and high-resolution transmission electron microscopy (HRTEM) techniques, Rietveld structure-refinements and scanning electron microscopy (SEM) techniques are described in Teertstra *et al.* (1997, 1998a, b).

## TERMINOLOGY

Triclinic rubicline was described by Teertstra *et al.* (1998a), and definition of the monoclinic Rb-analogue of high sanidine is expected in foreseeable future. However, identification of Rb-dominant feldspars as belonging to one or other species will likely be feasible for material from only a few localities. Our current experience shows that obtaining specific structural information on the state of (Al,Si) order is, in most cases, not possible by routine XRD methods because of the extremely fine grain-size of the Rb-rich feldspars, their compositional heterogeneity and intimate intergrowth with other minerals. Thus we use a simplified terminology based on chemical composition alone: K-feldspar as commonly used for alkali feldspar containing mainly K at the *M* site; rubidian K-feldspar or (K,Rb)-feldspar for Rb-bearing to Rb-rich K-feldspar with Rb ≤ K, and (potassic) Rb-feldspar or (Rb,K)-feldspar for phases with Rb > K; (K–Rb)-feldspar is used to indicate the entire series.

The varietal term *adularia* is used in its usual meaning: nonperthitic, Na-poor feldspar with typical short-prismatic to quasi-rhombohedral habit defined by the combination of {110} > {1$\bar{1}$0} > {001} forms. The term adularian feldspar is applied here to the same type of feldspar where it forms aggregates of anhedral grains.

## PARAGENETIC TYPES OF RUBIDIUM FELDSPARS

As indicated earlier, Rb-rich to Rb-dominant feldspars occur in three environments: (1) Rb-bearing blocky microcline perthite adjacent to pollucite bodies, (2) veins of nonperthitic, Rb-bearing, Na-poor microcline cross-cutting pollucite, and (3) clusters of adularia-type feldspar scattered in pollucite. There are three distinct modes of origin for the Rb-rich feldspars, all of them late and superimposed on the feldspars and pollucite quoted above: (i) exsolution (either from the blocky microcline perthite or from veins of nonperthitic microcline), (ii) solution – reprecipitation (from the same precursors), and (iii) replacement (of either the nonperthitic vein-type microcline or pollucite). General features of these processes and their products are given below under separate headings. However, the reader should consult the upcoming papers of Teertstra *et al.* (1998a, submitted, and in prep.), which document the complexity of late feldspar-generating processes in the full evolutionary context of local parageneses.

### *Exsolution from blocky and vein (K>Rb)-microcline*

Blocky (K,Na,Rb)-feldspar from the interior zones of highly fractionated pegmatites originally crystallized as a homogeneous disordered phase, and later underwent ordering of tetrahedral (Al,Si) and exsolution of perthitic albite (Martin 1982, Černý 1994). In the samples analyzed here, the separation of albite from its host is largely complete, and perthitic lamellae are commonly replaced by secondary K-feldspar or coarsened into irregular trains of granular albite. Textural evidence indicates that the exsolution and coarsening of albite preceded the formation of potassian Rb-feldspar.

Patchy distribution of Rb in the microcline phase of perthite is widespread, but the variations are largely too subtle for unambiguous genetic interpretation. However, local formation of veinlets of Rb-enriched feldspar is observed, parallel to the cleavage of the

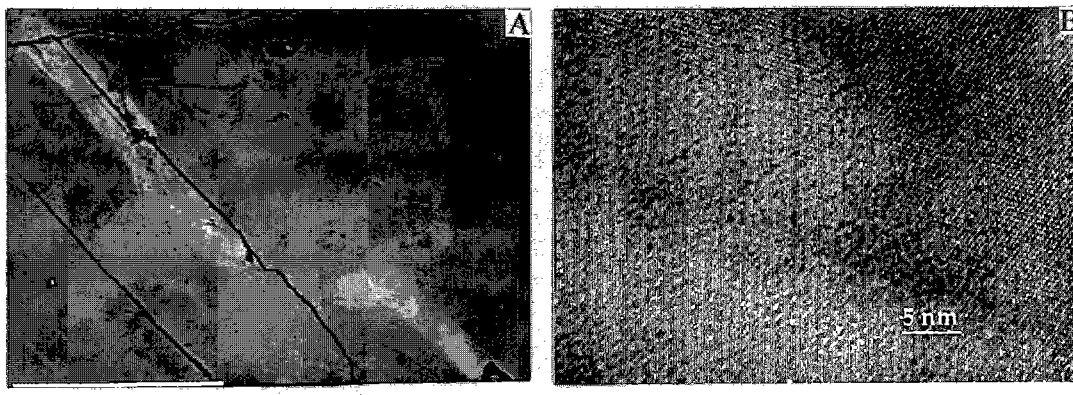


FIG. 1. A. Back-scattered electron (BSE) image of exsolution of Rb-rich feldspar (pale grey to white) from a Rb-bearing nonperthitic microcline (medium mottled grey), along an apparent zone of weakness in part parallel to cleavage, from the Rubellite pegmatite (Ontario). Note the dark grey areas of Rb-depleted microcline that flank the prominent segregations of Rb. The scale bar is 100 μm long. B. TEM micrograph of the structurally coherent interface between microcline (light) and rubicline (dark) from San Piero in Campo (modified from Teertstra *et al.* 1998a). The scale bar is 5 nm long.

host and associated with albite, and is attributed to exsolution of Rb-rich feldspar from a matrix that becomes K-enriched. Diffuse compositional gradients and traces of undisturbed cleavages suggest structural coherence with the host microcline. The proportions of Rb-enriched and Rb-depleted feldspar indicate local derivation from the Rb-bearing host; we do not observe any evidence for long-range migration of Rb-rich fluid. The patches and veinlets with variable Rb are associated with widespread and well-developed microporosity; pore density increases with the degree of redistribution of Rb. Textural coarsening of albite and (Rb,K)-feldspar was probably fluid-assisted. Explicit examples of exsolution of Rb-rich to Rb-dominant feldspar from the (K,Rb)-microcline phase of blocky perthitic feldspar come from the following occurrences of granitic pegmatite: Rubellite dike (Fig. 1A) and Tot Lake, in Ontario, Tanco, in Manitoba, Benson #1, in Zimbabwe, and Helikon, in Namibia (Table 1).

Veins of nonperthitic, twinned, triclinic (K,Rb)-feldspar in pollucite are largely Na-poor, but typically contain up to ~5 wt.% $Rb_2O$. The same patchy distribution of Rb and diffuse veining by Rb-rich feldspar are observed in these veins as in the blocky feldspar described above. Potassian Rb-feldspar is commonly adjacent to, and transitional into, patches of Rb-poor feldspar, suggesting variable degrees of exsolution of Rb-rich and K-rich phases. Structural coherence is documented by HRTEM images of nonperthitic microcline with patches of rubicline from San Piero in Campo, Elba (Fig. 1B; Teertstra *et al.* 1998a). Similar textures are found in samples from the Luolamäki pegmatite (Teertstra *et al.*, submitted). Texturally and compositionally analogous redistribution of Rb, suggestive of exsolution of rubicline from microcline, also is observed in veins of nonperthitic

TABLE 2. REPRESENTATIVE COMPOSITIONS OF (K-Rb)-FELDSPARS FORMED BY EXSOLUTION

| | Rubellite dike | | | San Piero in Campo | | |
|---|---|---|---|---|---|---|
| oxide | 1 | 2 | 3 | 4 | 5 | 6 |
| $SiO_2$ wt.% | 63.84 | 64.68 | 59.14 | 64.18 | 62.86 | 58.42 |
| $Al_2O_3$ | 17.84 | 17.89 | 17.42 | 18.23 | 18.52 | 15.84 |
| $P_2O_5$ | 0.26 | 0.04 | 0.03 | 0.06 | 0.25 | 0.00 |
| $Na_2O$ | 0.61 | 0.18 | 0.08 | 0.14 | 0.23 | 0.00 |
| $K_2O$ | 13.58 | 15.15 | 10.63 | 15.53 | 15.66 | 4.16 |
| $Rb_2O$ | 2.75 | 1.30 | 11.25 | 1.50 | 1.19 | 19.61 |
| $Cs_2O$ | 0.37 | 0.00 | 0.32 | 0.19 | 0.21 | 1.37 |
| SrO | 0.06 | 0.02 | 0.01 | 0.00 | 0.06 | 0.09 |
| BaO | 0.04 | 0.21 | 0.03 | 0.08 | 0.16 | 0.00 |
| Sum | 99.35 | 99.47 | 98.91 | 99.91 | 99.14 | 99.49 |
| | atomic contents based on 8 atoms of oxygen | | | | | |
| Si *apfu* | 3.004 | 3.018 | 2.963 | 2.996 | 2.962 | 3.032 |
| Al | 0.989 | 0.984 | 1.028 | 1.003 | 1.028 | 0.969 |
| P | 0.010 | 0.001 | 0.001 | 0.003 | 0.010 | 0.000 |
| Na | 0.056 | 0.016 | 0.008 | 0.013 | 0.021 | 0.000 |
| K | 0.815 | 0.902 | 0.680 | 0.925 | 0.941 | 0.276 |
| Rb | 0.083 | 0.039 | 0.363 | 0.046 | 0.036 | 0.654 |
| Cs | 0.007 | 0.000 | 0.007 | 0.004 | 0.004 | 0.030 |
| Sr | 0.002 | 0.001 | 0.000 | 0.000 | 0.001 | 0.003 |
| Ba | 0.001 | 0.004 | 0.001 | 0.001 | 0.003 | 0.000 |
| $\sum M$ | 0.964 | 0.962 | 1.059 | 0.989 | 1.006 | 0.963 |
| $M^+$ | 0.967 | 0.967 | 1.060 | 0.990 | 1.010 | 0.966 |
| $TO_2$ | 0.967 | 0.989 | 1.059 | 0.992 | 1.018 | 0.969 |
| $\sum T$ | 4.003 | 4.003 | 3.992 | 4.002 | 4.000 | 4.001 |

1: microcline precursor in blocky microcline-perthite
2: Rb-depleted microcline host
3: Rb-rich feldspar exsolved from 2 above
4: microcline precursor, non-perthitic veins in pollucite
5: Rb-depleted microcline host
6: rubicline exsolved from 5 above

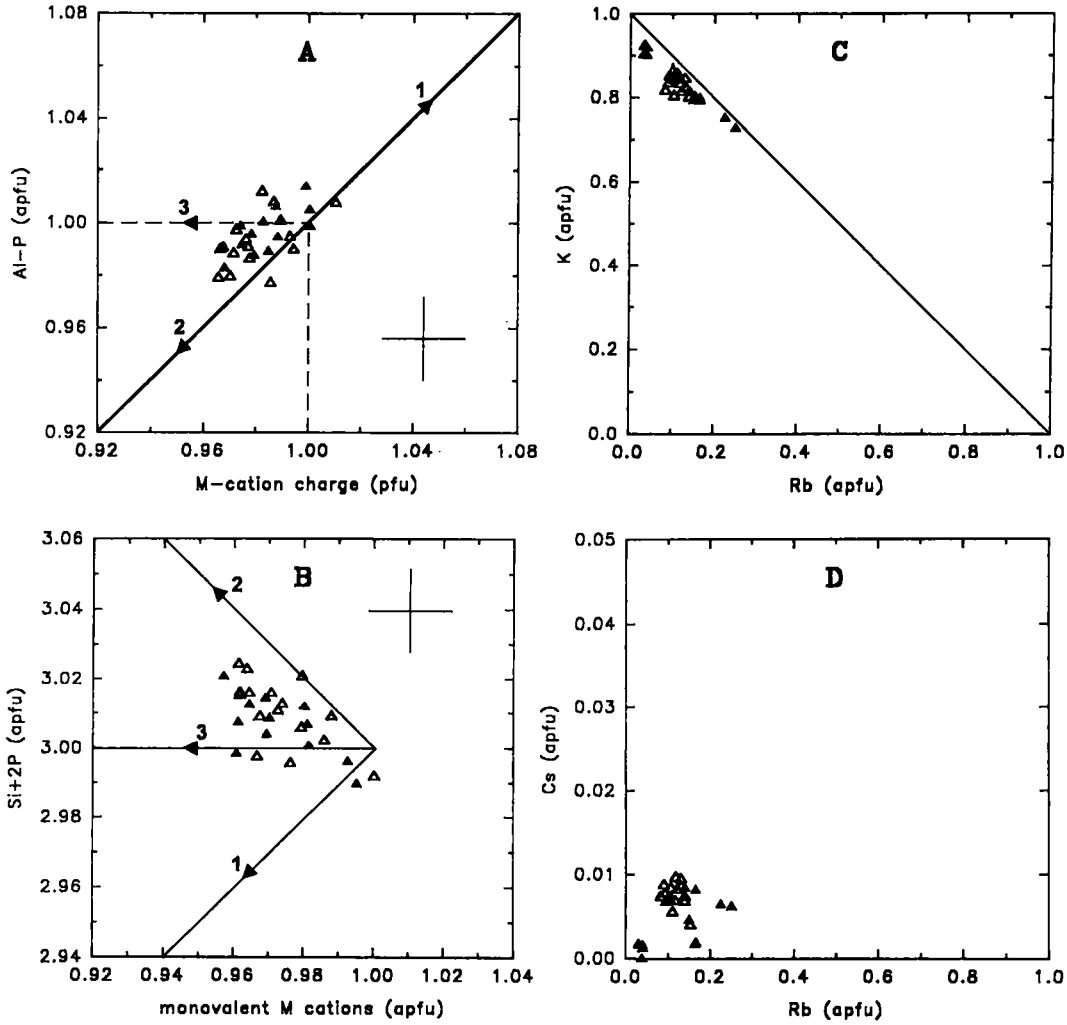


FIG. 2. Compositional relationships of (K–Rb)-feldspars generated by exsolution, from the Rubellite pegmatite. Parent nonperthitic vein microcline is shown by open triangles, and K- and Rb-enriched products of exsolution, by solid triangles; arrows indicate the plagioclase-type trend (1), the $\square Si_4O_8$ trend (2), and the trend of apparent cation deficiency, corresponding to incorporation of light elements (3). Data for all types of feldspar are spread along the $\square Si_4O_8$ trend, slightly shifted by incorporation of divalent cations. These substitutions, combined with low contents of Na, contribute to the slight deviation of (K + Rb) from ideality.

microcline from the Tanco granitic pegmatite, in the High Grade Dike, Manitoba, and at Viitaniemi, Finland (Table 1).

The chemical composition of the precursor feldspar is commonly characterized by substitution of significant $\square Si_4O_8$ (up to 5%; *e.g.*, Table 2, #1; Teertstra 1997). Feldspar that exhibits integral stoichiometry, such as the blocky (K,Rb)-feldspar from Red Cross Lake and the nonperthitic vein-type microcline from Kola, exsolves Rb-enriched phases only exceptionally. Many of the parent feldspar phases also show an apparent deficiency of *M* cations. Examples of compositions of the precursor feldspar and of the exsolved phases are shown in Table 2 and Figure 2.

*Solution – reprecipitation from (K>Rb)-microcline*

This process affects the same precursor phases as those exhibiting exsolution. Both blocky microcline perthite and vein-type nonperthitic microcline in

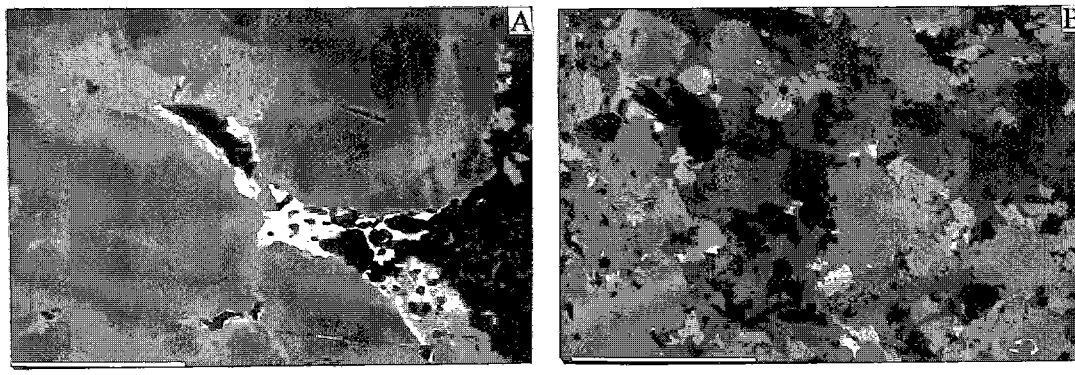


FIG. 3. BSE images of secondary feldspars generated by solution – reprecipitation. A. High Grade Dike pegmatite; the parent microcline, with an irregular distribution of Rb (mottled medium grey), is invaded by an aggregate of microporous (Rb,K)-feldspar (white) and end-member $Or_{100}$ adularian feldspar (black). B. Tanco pegmatite; the parent microcline (medium grey) is decomposed into an aggregate of (Rb,K)-feldspar (light grey to white), (K,Rb)-feldspar (dark grey) and cookeite (black). The scale bars are 100 μm long.

TABLE 3. REPRESENTATIVE COMPOSITIONS OF (K-Rb)-FELDSPARS FORMED BY SOLUTION-REPRECIPITATION

| | Tanco | | | High Grade Dike | | |
|---|---|---|---|---|---|---|
| oxide | 1 | 2 | 3 | 4 | 5 | 6 |
| $SiO_2$ wt.% | 63.61 | 64.37 | 56.82 | 63.65 | 64.68 | 57.75 |
| $Al_2O_3$ | 18.40 | 18.24 | 16.05 | 17.46 | 18.19 | 15.72 |
| $P_2O_5$ | 0.36 | 0.00 | 0.00 | 0.02 | 0.04 | 0.01 |
| $Na_2O$ | 0.22 | 0.03 | 0.00 | 0.10 | 0.01 | 0.00 |
| $K_2O$ | 14.88 | 16.83 | 2.68 | 13.79 | 16.68 | 2.33 |
| $Rb_2O$ | 2.50 | 0.00 | 23.75 | 3.95 | 0.00 | 24.07 |
| $Cs_2O$ | 0.273 | 0.03 | 0.56 | 0.35 | 0.02 | 0.57 |
| SrO | 0.09 | 0.07 | 0.10 | 0.02 | 0.01 | 0.07 |
| BaO | 0.10 | 0.08 | 0.00 | 0.00 | 0.04 | 0.00 |
| Sum | 100.53 | 99.77 | 99.96 | 99.44 | 99.96 | 100.66 |
| atomic contents based on 8 atoms of oxygen | | | | | | |
| Si *apfu* | 2.972 | 2.996 | 3.000 | 3.023 | 3.004 | 3.025 |
| Al | 1.013 | 0.999 | 0.999 | 0.977 | 0.996 | 0.973 |
| P | 0.014 | 0.000 | 0.000 | 0.001 | 0.000 | 0.000 |
| Na | 0.020 | 0.002 | 0.000 | 0.010 | 0.001 | 0.000 |
| K | 0.887 | 0.995 | 0.181 | 0.835 | 0.988 | 0.156 |
| Rb | 0.075 | 0.000 | 0.806 | 0.121 | 0.000 | 0.810 |
| Cs | 0.005 | 0.001 | 0.013 | 0.007 | 0.000 | 0.013 |
| Sr | 0.002 | 0.001 | 0.003 | 0.001 | 0.000 | 0.002 |
| Ba | 0.002 | 0.001 | 0.000 | 0.000 | 0.001 | 0.000 |
| $\sum M$ | 0.991 | 1.000 | 1.003 | 0.974 | 0.990 | 0.981 |
| $M^+$ | 0.996 | 1.003 | 1.005 | 0.976 | 0.992 | 0.983 |
| $TO_2$ | 1.000 | 1.002 | 0.999 | 0.976 | 0.994 | 0.973 |
| $\sum T$ | 3.999 | 3.995 | 3.999 | 4.001 | 4.000 | 3.998 |

1 and 4: precursor, non-perthitic microcline vein in pollucite
2 and 5: adularian K-feldspar intergrown with 3 and 6, respectively
3 and 6: (Rb,K)-feldspar intergrown with 2 and 5, respectively

pollucite show widespread, irregular, patchy and extensively microporous veins that consist of Rb-enriched to Rb-dominant feldspar, adularian K-feldspar and, locally, minor cookeite (Fig. 3). Very thin veinlets of (Rb,K)-feldspar, cross-cut by patches of adularian K-feldspar, are locally associated with these aggregates. The parent microcline commonly shows a heterogeneous distribution of Rb, which tends to accumulate along the margins of its grains (Fig. 3A). Optically, the microgranular aggregates of feldspars show a general lack of coherency either with the primary microcline or among the secondary grains of different chemical composition. The composition of the Rb-rich to Rb-dominant feldspar is variable, but that of the associated adularian K-feldspar is a uniform $Or_{100}$. The structural state of feldspars in the secondary aggregates could not be investigated because of their small size and compositional heterogeneity.

The mineral assemblage, aggregation and style of porosity of the secondary feldspars are distinctly different from those resulting from the exsolution described above. All the attributes of the granular aggregates indicate that the parent blocky or vein-type microcline broke down *via* dissolution along pathways of weakness and reprecipitation of a two-feldspar assemblage (± cookeite) facilitated by pore fluid. However, as in the case of exsolution, the ratio of the Rb-rich feldspar to the adularian K-feldspar, and the dispersion of isolated veins and patches of these feldspars, indicate local redistribution of K and Rb from the precursor microcline. There is no evidence of long-range transport of Rb or K. The best and most abundant examples of the solution – reprecipitation mechanism occur in samples from the Tanco and High Grade Dike pegmatites in Manitoba (Fig. 3), but were also observed in the following pegmatites: Red Cross Lake, Manitoba, Luolamäki, Finland, and Rubellite Dike, Ontario.

The solution – reprecipitation process is not selective in terms of (K,Rb)-precursors (Teertstra 1997). Blocky and vein microcline with integral stoichiometry or appreciable substitution toward

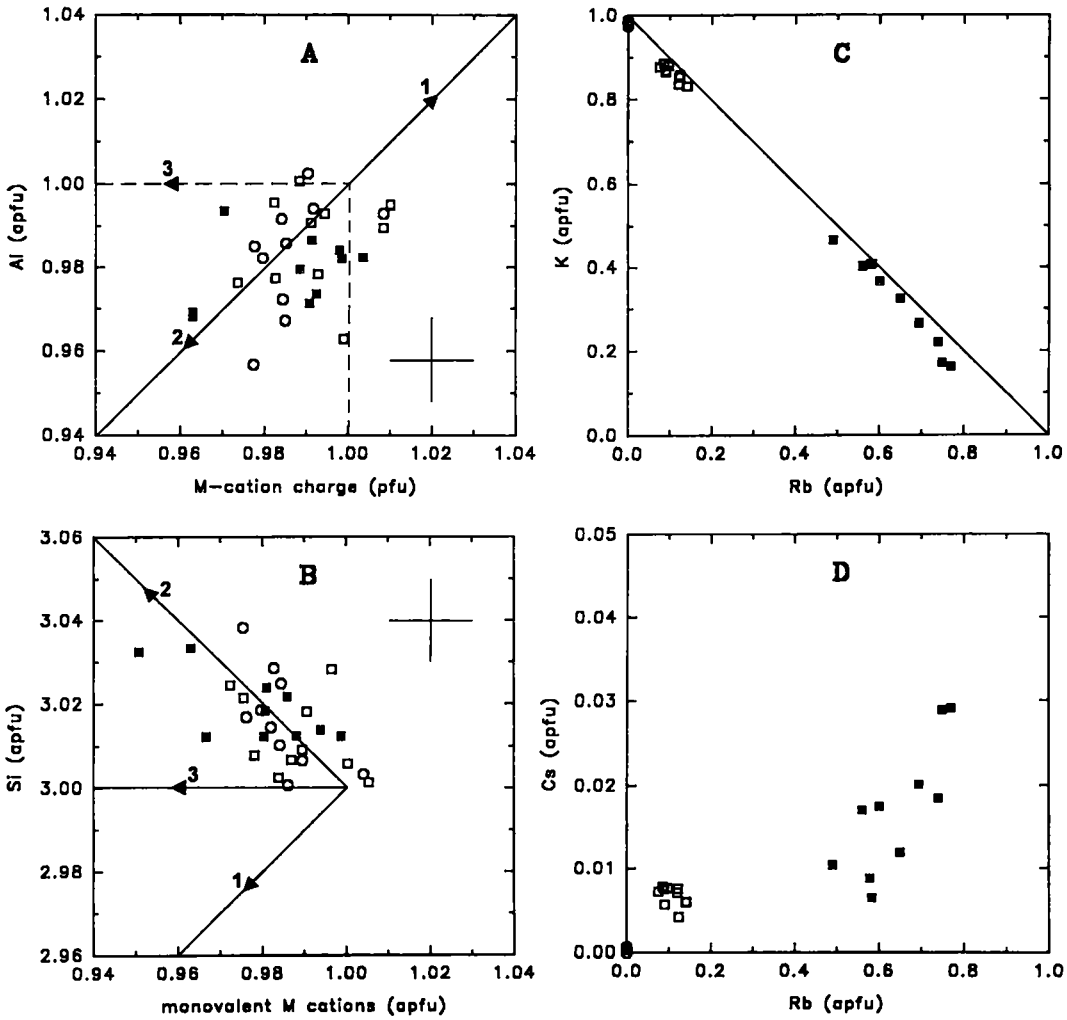


FIG. 4. Compositional relationships of (K–Rb)-feldspars generated by solution – reprecipitation, from the High Grade Dike pegmatite, Manitoba. Parent nonperthitic vein-type microcline is shown by open squares, Rb-enriched secondary feldspar, by solid squares, and associated $Or_{100}$ adularia, by open circles; trend lines as in Figure 2. All types of feldspar are P-free, and show incorporation of $\square Si_4O_8$ (up to 4 mol.%). Positive correlation is indicated for Rb and Cs.

$\square Si_4O_8$, low to high P content, and negligible to noticeable "deficit" of *M* cations all randomly undergo this style of breakdown. Table 3 shows representative chemical compositions of the precursor and secondary phases, and Figure 4 illustrates the compositional relationships for feldspars from the High Grade Dike.

*Replacement of pollucite by K- and (Rb,K)-feldspars*

Late-stage metasomatic replacement of early minerals (including feldspars, spodumene, petalite and pollucite) by adularian K-feldspar in granitic pegmatites is common. However, Rb-rich feldspars occur mainly in association with pollucite. These secondary feldspars constitute individual microscopic crystals of subhedral to euhedral adularia, or more commonly clusters 1 to (rarely) 3 mm in size. Round aggregates locally display radial structure (Fig. 5A). The feldspars form overgrowths on thin veinlets of white mica (Fig. 5B), or occur as isolated grains and clusters dispersed along fractures in pollucite. Closely associated but minor minerals include cookeite, apatite, albite, quartz, secondary end-member pollucite, calcite, fluorite, Rb- and Cs-enriched micas and clay minerals.

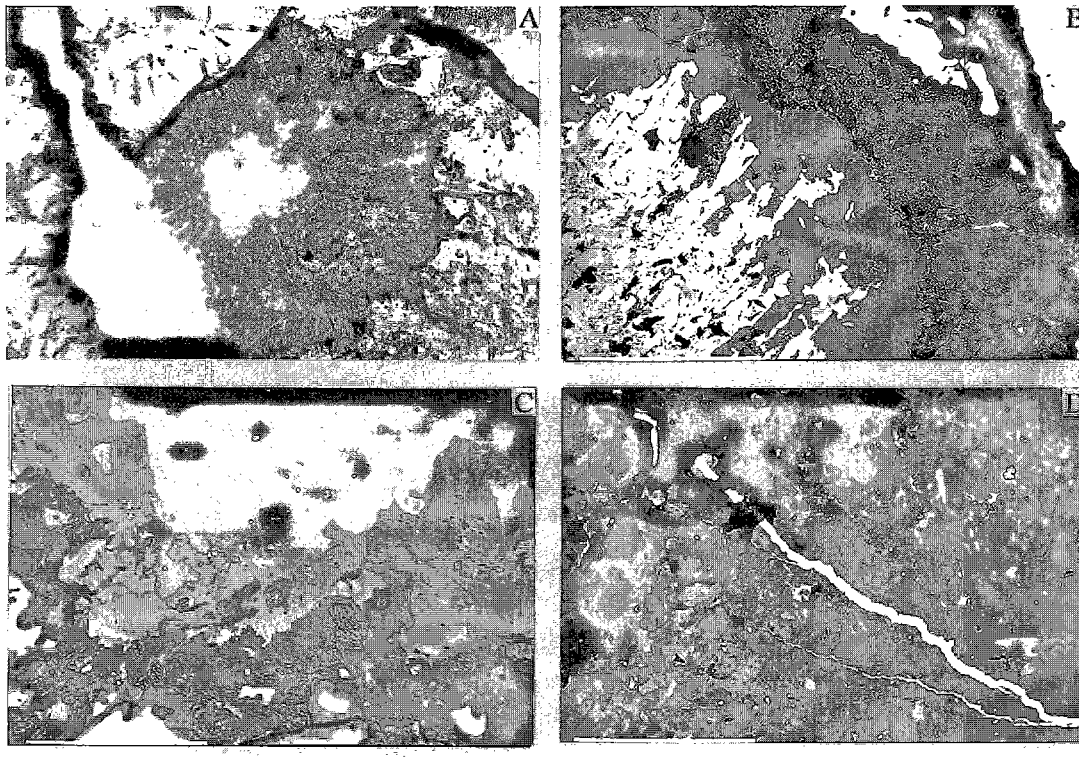


FIG. 5. Secondary feldspars generated by replacement of pollucite. A. A round, granular, subradial aggregate of adularian feldspar in pollucite ("dirty" white) from the Morrua pegmatite, Mozambique, adjacent to micaceous veinlets (black); optical photomicrograph in plane-polarized light. The vertical edge of the photograph is 0.5 mm long. B. BSE image of a zoned cluster from the Morrua pegmatite, with Rb-dominant feldspar in the core (off-white, left), overgrown first by clear and in turn microporous $Or_{100}$ adularian feldspar (grey), abutting pollucite (white, upper right); the pollucite is rimmed by secondary analcime (thin black rims) and cross-cut by a micaceous veinlet (black, subvertical). The scale bar is 200 μm long. C. BSE image of a zoned association from the Tot Lake pegmatite, in Ontario, with albite (black, top) overgrown by adularian feldspar of increasing Rb content (pale grey to white), rimmed by microporous $Or_{100}$, Rb-free adularian phase (medium grey) in contact with pollucite slightly converted to analcime (white grains along the bottom edge). The scale bar is 100 μm long. D. BSE image of a Rb-variable adularian feldspar (mottled grey) from the Tin Mountain pegmatite, in South Dakota, cross-cut by a veinlet of Rb-rich feldspar (white) and subsequently replaced by a Rb-free feldspar phase (black, upper left). The scale bar is 100 μm long.

The feldspars are compositionally heterogeneous, ranging from pure $Or_{100}$ to Rb-dominant phases with as much as 91 mol.% Rbf. At many localities, textural features of the feldspar aggregates show a gradual increase in Rb with progress of growth, but the distribution of Rb is uneven and strongly variable in adjacent grains (Fig. 5C). However, round radial aggregates in pollucite from Morrua, in Mozambique, Tot Lake, in Ontario, and, to a degree, Luolamäki, in Finland show an astonishingly uniform sequence of feldspar crystallization, from the centers of radial clusters outward: (1) low and variable Rb content in the core, grading to Rb-dominant compositions in the margins of the core, (2) a layer of non-porous adularian $Or_{100}$ feldspar, coated by (3) highly porous feldspar of the same composition, in contact with "analcimized" pollucite (Fig. 5B). Very thin veinlets of (Rb,K)-feldspar locally cross-cut these assemblages, and are themselves replaced by $Or_{100}$ adularian feldspar (Fig. 5D). Other localities that exhibit (K,Rb)- to (Rb,K)-feldspar metasomatic after pollucite are as follows: High Grade Dike in Manitoba, Valor in Quebec, Kola Peninsula in Russia, San Piero in Campo, on Elba, Old Tom in Maine, Himalaya in California, Tin Mountain in South Dakota, Nyköpingsgruvan North in Sweden, Bikita in Zimbabwe, Helikon in Namibia, and an unspecified pegmatite in eastern Siberia (Table 1).

The structural state of the Rb-dominant adularian feldspar replacing pollucite is so far undetermined. However, XRD examination revealed a highly disordered

TABLE 4. REPRESENTATIVE COMPOSITIONS OF (K-Rb)-FELDSPARS FORMED BY REPLACEMENT OF POLLUCITE

| | Tot Lake | | | Tin Mountain | | |
|---|---|---|---|---|---|---|
| oxide | 1 | 2 | 3 | 4 | 5 | 6 |
| $SiO_2$ wt.% | 62.88 | 58.24 | 64.66 | 63.68 | 58.10 | 64.66 |
| $Al_2O_3$ | 18.06 | 16.83 | 17.86 | 17.67 | 16.31 | 18.32 |
| $P_2O_5$ | 0.00 | 0.00 | 0.00 | 0.00 | 0.02 | 0.01 |
| $Na_2O$ | 0.10 | 0.00 | 0.02 | 0.00 | 0.00 | 0.01 |
| $K_2O$ | 14.93 | 7.06 | 16.24 | 13.72 | 4.51 | 16.95 |
| $Rb_2O$ | 2.83 | 16.58 | 0.00 | 4.88 | 19.24 | 0.00 |
| $Cs_2O$ | 0.14 | 0.39 | 0.00 | 0.11 | 1.21 | 0.00 |
| SrO | 0.04 | 0.00 | 0.00 | 0.00 | 0.11 | 0.10 |
| BaO | 0.00 | 0.00 | 0.17 | 0.00 | 0.00 | 0.00 |
| Sum | 98.98 | 99.10 | 98.95 | 100.10 | 99.51 | 100.06 |
| | atomic contents based on 8 atoms of oxygen | | | | | |
| Si *apfu* | 2.988 | 2.983 | 3.018 | 3.016 | 3.009 | 2.997 |
| Al | 1.012 | 1.015 | 0.982 | 0.986 | 0.996 | 1.001 |
| P | 0.000 | 0.000 | 0.000 | 0.000 | 0.001 | 0.000 |
| Na | 0.009 | 0.000 | 0.003 | 0.000 | 0.000 | 0.001 |
| K | 0.905 | 0.461 | 0.967 | 0.829 | 0.298 | 1.002 |
| Rb | 0.086 | 0.545 | 0.000 | 0.148 | 0.641 | 0.000 |
| Cs | 0.003 | 0.009 | 0.000 | 0.002 | 0.027 | 0.000 |
| Sr | 0.001 | 0.000 | 0.000 | 0.000 | 0.003 | 0.003 |
| Ba | 0.000 | 0.000 | 0.003 | 0.000 | 0.000 | 0.000 |
| $\sum M$ | 1.004 | 1.015 | 0.973 | 0.979 | 0.969 | 1.006 |
| $M^+$ | 1.005 | 1.015 | 0.976 | 0.979 | 0.972 | 1.009 |
| $TO_2$ | 1.012 | 1.015 | 0.982 | 0.986 | 0.995 | 1.001 |
| $\sum T$ | 4.000 | 3.998 | 4.000 | 4.002 | 4.006 | 3.998 |

1 and 4: Rb-poor adularian feldspar
2 and 5: Rb-dominant adularian feldspar
3 and 6: $Or_{100}$ adularia associated with 2 and 5, respectively

state of the closely associated potassic phase at several localities: the High Grade Dike adularian K-feldspar proved to be a good match to the Tanco adularia, representative of a structural and compositional end-member K-feldspar (Teertstra *et al.*, submitted). Thus it is conceivable that the Rb-dominant feldspar, crystallized concurrently with the high sanidine potassic adularia, also is highly disordered. Under identical conditions of precipitation, the ionic radius of Rb should favor (Al,Si) disorder even more than the smaller K.

Table 4 presents representative compositions of the metasomatic K- and (Rb,K)-feldspars from the Tot Lake and Tin Mountain pegmatites, and Figure 6 shows compositional variations at Luolamäki. In general, the metasomatic feldspars from diverse localities typically are very poor in Na and divalent cations, and P is undetectable. Stoichiometry is variable, from ideal integral (Table 4, #6) to silica-enriched owing to $\square Si_4O_8$ substitution (Table 4, #3 and 4); *M*-cation-"deficient" compositions, suggestive of incorporation of light elements, also are encountered (Table 4, #3 and 5).

## DISCUSSION

### *Origin of (Rb,K)-feldspars and associated phases*

The stage for the formation of the (Rb,K)-feldspars was set during the conclusion of magmatic crystallization of the host pegmatites. Blocky (K,Na,Rb)-feldspar, crystallized as a homogeneous disordered phase, is among the latest magmatic precipitates near cores of the pegmatites (Černý 1994), followed by primary pollucite as a near-solidus product (Henderson & Manning 1984, London *et al.* 1998). At ~450°C, subsolidus conversion to microcline was followed closely by exsolution of albite, approximately concurrently with initial breakdown of pollucite into Na,Si- and Cs,Al-enriched forms (Fig. 7; *e.g.*, Teertstra & Černý 1995, 1997). Veining of pollucite by initially monoclinic, Na-poor K-feldspar, converted soon after its precipitation to nonperthitic microcline, must have taken place in this temperature range.

Exsolution of (Rb,K)-feldspar from blocky perthitic microcline and nonperthitic vein microcline followed exsolution of perthitic albite (Fig. 1), apparently because of the slower diffusion of Rb relative to Na. The exsolution does not resemble the lamellar form commonly encountered in perthite. The most probable reason for the irregular shape of the Rb-enriched feldspar, and its diffuse transitions into the K-dominant host, is the very small dimensional and angular difference between the unit cells of end-member microcline and rubicline, and between high sanidine and its Rb-analogue (*cf.* Pentinghaus & Henderson 1979, McMillan *et al.* 1980, Černý *et al.* 1985, Teertstra 1997). The differences are, of course, still smaller between intermediate members of the (K–Rb) series that constitute most of the exsolved pairs of feldspars. The exsolution amounts to small-scale migration of alkalis in an aluminosilicate framework that shows only very minor distortion; it preserves perfect coherence between the exsolved phases. However, it is possible that the present texture of the intergrowth could have been modified by reaction with late aqueous fluids.

Substitution toward $\square Si_4O_8$ in the precursor feldspar apparently promotes the exsolution process. Exsolution of (Rb,K)-feldspar is very limited in samples of integral stoichiometry, despite their high Rb content. Enhanced microporosity of the exsolved feldspars indicates assistance of a fluid phase during the process.

During the solution – reprecipitation reaction of blocky microcline perthite and nonperthitic microcline, the role of late fluids was evidently intense, and should probably be classified as hydrothermal rather than deuteric. The cocrystallized (Rb,K)-feldspar and $Or_{100}$ adularian feldspar are extensively microporous and associated with locally abundant cookeite (Figs. 3A, B).

The timing of the above process probably coincided with metasomatic replacement of pollucite by adularian (K,Rb)- to (Rb,K)-feldspar and $Or_{100}$ adularia, more or

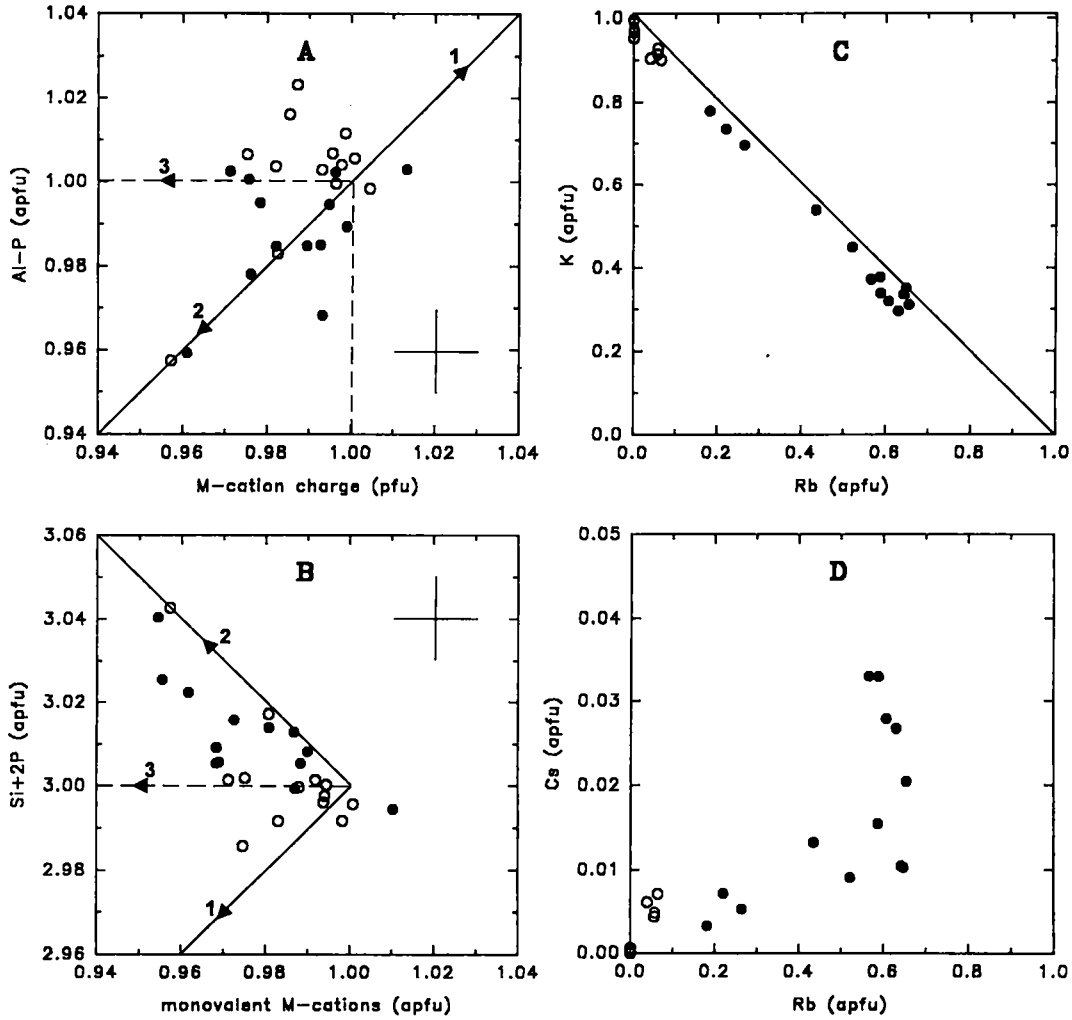


FIG. 6. Compositional relationships of (K–Rb)-feldspars generated by replacement of pollucite, from the Luolamäki granitic pegmatite, in Finland. Rubidium-rich (solid dots) and associated Rb-free (open circles) adularian feldspar, are shown with trend lines as in Figure 2. The Rb-rich feldspar shows incorporation of $\square Si_4O_8$ (up to 4 mol.%), and both feldspars have an apparent deficiency in *M* cations attaining a maximum of 4 at.%. These trends combine with the effects of minor Na and Cs substitution for (K,Rb) to reduce the sum of (K + Rb) to less than unity. The concentration of cesium is positively correlated with that of Rb.

less associated with veining of pollucite by muscovite and spodumene (Figs. 5A, B). Association of these feldspars with end-member pollucite, which forms in the final stages of pollucite re-equilibration (Teertstra & Černý 1995), indicates a low-temperature origin at about 250°C, followed only by alteration of pollucite to analcime and of most of the silicates to clays.

*The Kfs – Rbf solvus*

K- and Rb-feldspar form a continuous solid-solution series at 400°C (Volfinger 1976, Lagache 1984), but reactions become extremely sluggish at lower temperatures, and experimental work is impractical (M. Lagache, pers. commun. 1994). Our study of natural feldspars of low-temperature origin shows that a solvus must exist below 400°C: exsolution in early generations of (K,Rb)-feldspar (Fig. 2C), coprecipitation of Rb- and K-enriched feldspar after dissolution of the same early phases (Fig. 4C), and metasomatism of pollucite by coexisting (Rb,K)- and K-feldspar (Fig. 6C) all indicate the existence of a miscibility gap. The possibility of a solvus is also indicated by moderately positive values for the Gibbs free energy of mixing of (K–Rb)-feldspar, determined experimentally by Lagache & Sabatier (1973).

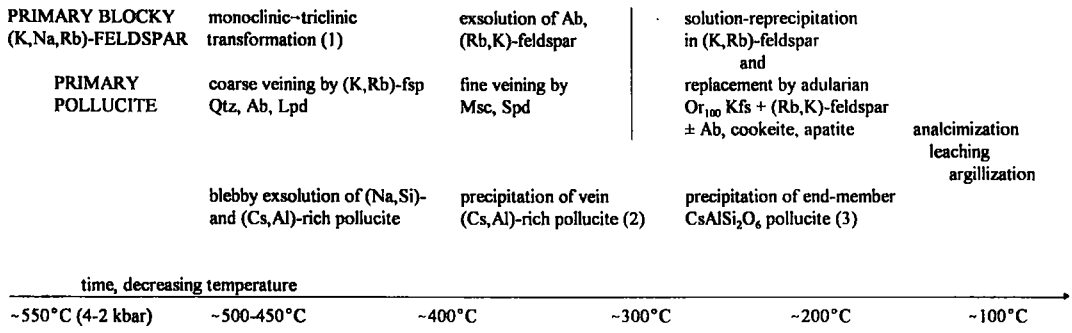


FIG. 7. Sequences of phase transformation, re-equilibration and alteration of alkali feldspar and pollucite, approximately correlated with decreasing temperature. Additional information may be found in (1) Brown & Parsons (1989), (2) Teertstra & Černý (1995, 1997), Teertstra *et al.* (1996b), (3) Teertstra & Černý (1995).

Some of our data show that end-member K-feldspar coprecipitates in equilibrium textures with a ~80 mol.% Rb-feldspar (*e.g.*, Fig. 4C) at ~250 to 150°C. However, compositions in the range of 50 to 80 mol.% Rbf are rather common, and they show zoning and patchy distribution of Rb indicative of disequilibrium crystallization (Figs. 4C, 6C). Reactions of (K–Rb)-feldspars are evidently as sluggish in natural low-temperature environments as in experimental work. The compositional heterogeneity of the low-temperature, microscopic-scale assemblages of (K–Rb)-feldspars indicates that the products of exsolution, reprecipitation and metasomatism were never driven to compositional equilibrium.

In contrast, coexisting albite and K-feldspar also are common in some of the secondary assemblages, invariably with end-member compositions, $Ab_{100}$ and $Or_{100}$. The large positive values for the Gibbs free energy of mixing in the K–Na feldspar series correlate with the observed equilibrium textures and compositions, as expected for a system with a solvus cresting at high temperatures.

### *Structural state of the low-temperature (K–Rb)-feldspars*

The highly (Al,Si)-ordered state of (Rb,K)-feldspar exsolved from (K,Rb)-microcline is documented experimentally for the type rubicline, and is strongly suspected in other cases of Rb-feldspar hosted by microcline. The structural state is evidently maintained from the compositionally homogeneous, (Al,Si)-ordered precursor to the exsolved Rb-enriched and K-enriched domains (with slight modifications of the unit-cell parameters), in a process analogous to synthesis of triclinic Rb-feldspar by cation exchange from microcline (*e.g.*, McMillan *et al.* 1980).

In contrast, the metasomatic $Or_{100}$ adularia in pollucite is typically a totally disordered high sanidine (Teertstra *et al.* 1998b), and the same structural state can be expected for the associated (Rb,K)-feldspar, in part because of the larger radius of Rb. No direct information on structural state was obtained for either of the feldspars formed by solution – reprecipitation. However, disordered structures are expected, as they formed in about the same P–T regime as the metasomatic feldspars in pollucite, in granular aggregates that do not exhibit any coherence with their triclinic precursor.

### *Crystal-chemical aspects of the (Rb,K)-feldspar and associated feldspars*

The microcline perthite and nonperthitic microcline precursors, proven free of quartz by XRD examination, show incorporation of up to 5 mol.% $\square Si_4O_8$ (*e.g.*, Figs. 2A, B, 4A, B). This substitution, so far not reported in microcline, is widespread in microcline from the highly hydrous environment of complex granitic pegmatites (unpubl. data of DKT). This substitution provides a mechanism for structural incorporation of $H_2O$, which may aid in the conversion to a triclinic polymorph (Waldron *et al.* 1993). The *M*-site vacancies may also promote alkali migration during exsolution, as feldspars with integral stoichiometry but elevated Rb show minimal evidence for an exsolution style of re-equilibration (*e.g.*, blocky perthitic alkali feldspar from Red Cross Lake and vein microcline from Kola Peninsula). Additional work, beyond the scope of this study, is required for quantitative determination of $H_2O$ and rates of alkali diffusion in feldspars that exhibit the $\square Si_4O_8$ substitution.

The secondary (K–Rb)-feldspars lie close to the join $KAlSi_3O_8 - RbAlSi_3O_8$ and have up to 26.2 wt.% $Rb_2O$ (91 mol.% Rbf) and 1.5 wt.% $Cs_2O$ (3 mol.% Csf). In general, the analytical results conform to the feldspar formula. However, compared to the Eifel standard (Teertstra *et al.* 1998b), larger compositional scatter is

observed for the $M$, $T$ and oxide sums, even for samples in which mean values of $M^+$ and $TO_2^-$ are equal. This increased scatter of results about values expected for ideal stoichiometry is independent of any particular mechanism of substitution. Random scatter is minimal and approximately equal to 1% (4σ) in the standard (Teertstra *et al.* 1998b) and in other feldspars that are optically transparent and largely non-porous. In contrast, random scatter is greatest in turbid and highly porous phases, and is attributed to an overlap of the analyzed volume with micropores: fluid (± solid-inclusion)-filled micropores typically occupy ~1.5 vol.% of turbid feldspar and have a density of up to $10^9$ mm$^{-3}$ (Walker *et al.* 1995). However, the random scatter does not obliterate, or invalidate, the trends deviating from integral stoichiometry, which are still easily discernible (*e.g.*, Figs. 6A, B).

Except on a local scale, substitution of divalent alkaline earths or Fe in the feldspars examined is negligible, and compositions do not lie along the trend defined by a plagioclase-type substitution. Exsolution of albite is nearly complete in the blocky (K,Rb)-precursor, and its K-phase contains less than 0.5 wt.% $Na_2O$, whereas later feldspars tend to be entirely Na-free. The Rb-rich part of the (K–Rb)-feldspar series (with more than ~10 mol.% Rbf) is Ca-free, with negligible to undetectable concentrations of Na, Sr, Ba, Fe or P, but Cs generally increases with Rb (Figs. 2D, 4D, 6D). An absence of B is indicated by values of $M^+$ less than $TO_2^-$, and $\Sigma T$ values, of 4.000 ± 0.002 *apfu*, but substitution of light-element $M$ cations may attain 4 at.% (Figs. 6A, B). The $M$-cation "deficiency" seems to be characteristic of localities in which the early feldspar contains $P_2O_5$. Phosphorus incorporation *via* the berlinite substitution is important mainly in the early generations of K-feldspar, and is largely absent in later generations.

## Conclusions

(1) Late, low-temperature, fine-grained Rb-feldspar was found in twelve highly fractionated pollucite-bearing pegmatites, and K-dominant but Rb-rich feldspar was studied at an additional twenty-one localities. Paragenetic considerations indicate that a (Rb,K)-feldspar may be present at a significant number of rare-element granitic pegmatites worldwide, particularly (but not necessarily) associated with pollucite.

(2) Compositions of these feldspars lie close to the join $KAlSi_3O_8$ – $RbAlSi_3O_8$, with up to 26.2 wt.% $Rb_2O$ (91 mol.% Rbf) and 1.5 wt.% $Cs_2O$ (3 mol.% Csf). Na and Ca contents are negligible; the main deviation from stoichiometry is due to incorporation of a few % of $\square Si_4O_8$ and light-element $M$ cations.

(3) Rubidium feldspars occur in three associations: (1) blocky microcline(-perthite) of internal pegmatite zones commonly adjacent to pollucite bodies, (2) late veins of nonperthitic microcline cross-cutting pollucite, and (3) adularian feldspar in pollucite. Three genetic mechanisms produce Rb-feldspars: (i) exsolution from (K,Rb)-precursors, (ii) re-equilibration by solution – reprecipitation of (K,Rb)-precursors, and (iii) metasomatic replacement of pollucite by adularian feldspar.

(4) Exsolution operates typically in early (K,Rb)-feldspars that have a significant level of $\square Si_4O_8$, and is followed by coarsening assisted by deuteric processes. Structural coherence of the exsolved Rb-dominant phases with the triclinic host is documented in one case and strongly suggested in others. The exsolution is apparently promoted by migration of $M$-site vacancies, and (Al,Si)-ordering is possibly catalyzed by partial occupancy of □ by $H_2O$.

(5) Late-precipitating adularian feldspars are highly disordered in the case of $Or_{100}$, and likely so for the coexisting $Rbf_{\sim 80}$ phase. These feldspars form owing to the presence of a solvus cresting at less than 400°C. Compositionally zoned and generally heterogeneous feldspars in the range $Rbf_{50}$ to $Rbf_{80}$ are common, but are probably metastable because of slow diffusion of Rb at low temperatures; most reactions were evidently arrested before completion.

(6) The $\square Si_4O_8$ and light-element substitutions, recorded during the present study, are in sharp contrast with the perfect integral stoichiometry of numerous feldspars from granites and other pegmatites that were studied concurrently. Further work is required to establish the distribution of these substitutions, and their links with other attributes of feldspar composition, such as the berlinite substitution $(AlP)Si_{-2}$.

## Acknowledgements

This research was supported by NSERC Research and Major Installation Grants to PČ, by NSERC Research, Equipment and Infrastructure Grants to FCH and by a University of Manitoba Duff Roblin Fellowship to DKT. Field work was in part also financed by the Canada – Manitoba Mineral Development Agreement (1984–1989). Our thanks go to the late O. von Knorring, the late J. Donner, M.A. Cooper, and K.J. Neuvonen for some of the feldspar samples, to C.M.B. Henderson for the Rb standard, and to H. Wondratschek for the Eifel sanidine. The thorough constructive reviews by C.M.B. Henderson and I. Parsons, and the editorial work of R.F. Martin helped extensively to streamline and focus the presentation.

## References

Brown, W.L. & Parsons, I. (1989): Alkali feldspars: ordering rates, phase transformations and behaviour diagrams for igneous rocks. *Mineral. Mag.* **53**, 25-42.

Bruno, E. & Pentinghaus, H. (1974): Substitution of cations in natural and synthetic feldspars. *In* The Feldspars (W.S.

Mackenzie & J. Zussman, eds.). Manchester University Press, Manchester, U.K. (574-609).

ČERNÝ, P. (1991): Rare-element granitic pegmatites. I. Anatomy and internal evolution of pegmatite deposits. *Geosci. Can.* **18**, 49-67.

_____ (1994): Evolution of feldspars in granitic pegmatites. *In* Feldspars and Their Reactions (I. Parsons, ed.). Reidel Publ. Co., Dordrecht, The Netherlands (501-540).

_____, PENTINGHAUS, H. & MACEK, J.J. (1985): Rubidian microcline from Red Cross Lake, northeastern Manitoba. *Bull. Geol. Soc. Finland* **57**, 217-230.

GASPERIN, M. (1971): Structure cristalline de $RbAlSi_3O_8$. *Acta Crystallogr.* **B27**, 854-855.

GHÉLIS, M. & GASPERIN, M. (1970): Evolution des paramètres dans le système $KAlSi_3O_8$ – $RbAlSi_3O_8$. *C.R. Acad. Sci. Paris* **271**, *Sér.* **D**, 1928-1929.

HENDERSON, C.M.B. & MANNING, D.A.C. (1984): The effect of Cs on phase relations in the granite system: stability of pollucite. *In* Progress in Experimental Petrology, sixth progress report of research supported by N.E.R.C., 1981–1984. *Nat. Env. Res. Council (UK) Publ. Ser. D* **25**, 41-42.

LAGACHE, M. (1984): The exchange equilibrium distributions of alkali and alkaline-earth elements between feldspars and hydrothermal solutions. *In* Feldspars and Feldspathoids (W.L. Brown, ed.). Reidel Publ. Co., Dordrecht, The Netherlands (247-279).

_____ & SABATIER, G. (1973): Distribution des éléments Na, K, Rb et Cs à l'état de trace entre feldspaths alcalins et solutions hydrothermales à 650°C, 1 kbar: données expérimentales et interprétation thermodynamique. *Geochim. Cosmochim. Acta* **37**, 2617-2640.

LONDON, D., ČERNÝ, P., LOOMIS, J.L. & PAN, J.J. (1990): Phosphorus in alkali feldspars of rare-element granitic pegmatites. *Can. Mineral.* **28**, 771-786.

_____, MORGAN, G.B., VI & ICENHOWER, J. (1998): Stability and solubility of pollucite in the granite system at 200 MPa $H_2O$. *Can. Mineral.* **36**, 497-510.

MARTIN, R.F. (1982): Quartz and the feldspars. *In* Granitic Pegmatites in Science and Industry (P. Černý, ed.). *Mineral. Assoc. Can., Short-Course Handbook* **8**, 41-62.

MCMILLAN, P.F., BROWN, W.L. & OPENSHAW, R.E. (1980): The unit-cell parameters of an ordered K–Rb alkali feldspar series. *Am.Mineral.* **65**, 458-464.

PENTINGHAUS, H. & HENDERSON, C.M.B. (1979): Rubidium-aluminosilikat-Feldspat ($RbAlSi_3O_8$): Stabilität, strukturelle Zustande und Schmelzverhalten; chemische und thermische Ausdehnung des ($AlSi_3O_8$)-Gerüstes. *Fortschr. Mineral.* **57**, 119-120.

POUCHOU, J.-L. & PICHOIR, F. (1985): "PAP" (phi-rho-Z) procedure for improved quantitative microanalysis. *In* Microbeam Analysis (J.T. Armstrong, ed.). San Francisco Press, San Francisco, California (104-106).

TEERTSTRA, D.K. (1997): *Reactions of (K–Rb) Feldspars from Rare-Element Granitic Pegmatites.* Ph.D. thesis, Univ. Manitoba, Winnipeg, Manitoba.

_____ & ČERNÝ, P. (1993): Rubidian adularia as an alteration product of pollucite, Morrua mine, Mozambique. *NATO – Adv. Study Inst. on Feldspars and Their Reactions, Abstr., poster* 9.

_____ & _____ (1994): Compositional heterogeneity of K,Rb-feldspars from highly fractionated granitic pegmatites. *Geol. Assoc. Can. – Mineral. Assoc. Can., Program Abstr.* **19**, 110.

_____ & _____ (1995): First natural occurrences of end-member pollucite: a product of low-temperature reequilibration. *Eur. J. Mineral.* **7**, 1137-1148.

_____ & _____ (1997): The compositional evolution of pollucite from African granitic pegmatites. *J. Afr. Earth Sci.* **25**, 317-331.

_____, _____ & HAWTHORNE, F.C. (1996a): The composition of subsolidus K,Rb-feldspars, Morrua pegmatite, Alto Ligonha, Mozambique. *Geol. Assoc. Can. – Mineral. Assoc. Can., Program Abstr.* **21**, A94.

_____, _____ & _____ (1997): Rubidium-rich feldspars in a granitic pegmatite from the Kola Peninsula, Russia. *Can. Mineral.* **35**, 1277-1281.

_____, _____, _____, PIER, J., WANG, LU-MIN & EWING, R.C. (1998a): Rubicline, a new feldspar from San Piero in Campo, Elba, Italy. *Am. Mineral.* **83** (in press).

_____, _____, LANGHOF, J., SMEDS, S.-A. & GRENSMAN, F. (1996b): Pollucite in Sweden: occurrences, crystal chemistry, petrology and subsolidus history. *GFF (Geol. Fören. Stockholm Förh.)* **118**, 141-149.

_____, HAWTHORNE, F.C. & ČERNÝ, P. (1998b): Identification of normal and anomalous compositions of minerals by electron-microprobe analysis: K-rich feldspar as a case study. *Can. Mineral.* **36**, 87-96.

_____, LAHTI, S.I., ALVIOLA, R. & ČERNÝ, P. (1993): Pollucite and its alteration in Finnish pegmatites. *Geol. Surv. Finland Bull.* **368**, 1-39.

VOLFINGER, M. (1976): Effet de la température sur les distributions de Na, Rb et Cs entre la sanidine, la muscovite, la phlogopite et une solution hydrothermale sous une pression de 1 kbar. *Geochim. Cosmochim. Acta* **40**, 267-282.

VONCKEN, J.H.L., KONINGS, R.J.M., VAN DER EERDEN, A.M.J., JANSEN, J.B.H., SCHUILING, R.D. & WOENSDREGT, C.F. (1993): Crystal morphology and X-ray powder diffraction of the Rb-analogue of high sanidine, $RbAlSi_3O_8$. *Neues Jahrb. Mineral., Monatsh.*, 10-16.

WALDRON, K., PARSONS, I. & BROWN, W.L. (1993): Solution – redeposition and the orthoclase – microcline transformation: evidence from granulites and relevance to $^{18}O$ exchange. *Mineral. Mag.* **57**, 687-695.

WALKER, F.D.L., LEE, M.R. & PARSONS, I. (1995): Micropores and micropermeable texture in alkali feldspars: geochemical and geophysical implications. *Mineral. Mag.* **59**, 505-534.

WIETZE, R. & WISWANATHAN, K. (1971): Rubidium-Plagioklas durch Kationenaustauch. *Fortschr. Mineral.* **49**, 63.

*Received May 13, 1997, revised manuscript accepted April 27, 1998.*